Journal of
Advanced Manufacturing Science and Technology
jamst@jamstjournal.com;jamst2020@126.com
www.jamstjournal.com

Micro electro discharge milling of titanium super alloy: Analysis of material removal rate and surface roughness

Mohammad Yeakub ALI[a,*], Mohamed Abd RAHMAN[b], Muhamad Faizal Mohd KARIN[b], Mohd Saifuddin AMINDDIN[b], Seri Rahayu YA'AKUB[a], Muataz Hazza Al HAZZA[c] Abdul Md MAZID[d]

[a] *Mechanical Engineering Programme Area, Universiti Teknologi Brunei, Gadong BE1410, Brunei Darussalam*
[b] *Department of Manufacturing and Materials Engineering, International Islamic University Malaysia, Kuala Lumpur 50728, Malaysia*
[c] *Mechanical Engineering Department, American University of Ras Al Khaimah, Ras Al Khaimah PO Box 10021, United Arab Emirates*
[d] *School of Engineering and Technology, Central Queensland University Australia, Melbourne VIC3000, Australia*

Received 9 May 2024; revised 17 June 2024; accepted 11 July 2024; Available online 24 July 2024

Abstract: This paper presents the machinability of titanium super alloy Ti-6Al-4V using micro electro discharge milling (Micro-ED Milling). Material removal rate (MRR), tool wear rate (TWR) and surface roughness were analysed using L18 orthogonal arrays of experiment. Based on analysis of variance (ANOVA) and signal-to-noise (S/N) ratio, empirical models have been developed. Optimum values of micro-ED milling parameters to achieve maximum MRR, minimum TWR and minimum surface roughness (R_a and R_y) were obtained. The optimum parameters were found to be 100 nF capacitance and 80 V gap voltage which leveraged 57.8 μg/s MRR and 0.96 μg/s TWR with 90% desirability. In addition, the optimum parameters for the minimum surface roughness were found to be 1 nF capacitance and 80 V gap voltage which produced 0.086 μm R_a and 0.63 μm R_y with 99% desirability. Experimental studies were conducted using optimum micro-ED milling parameters to validate the results. It was found that the predicted values were within 10% of the experimental values.

Keywords: Surface roughness; Material removal rate; Tool wear rate; Titanium alloy; Micro-EDM

1. Introduction

As a micromachining technique, micro electrical discharge machining is emerging as a potential cost savings alternative. This process can produce high aspect ratio sub-millimetre sized components with high accuracy and surface finish for applications in microelectromechanical systems[1]. In addition, this is a non-traditional machining process where tool and workpiece have no physical contact and can machine any conductive material regardless of their hardness[2-3]. EDM is an advanced manufacturing process developed in the late 1940s[4]. The EDM may appear to be a relatively mature process, but development is continuing, including its application to productivity improvements as well as specialized techniques such as micro texturing. Examples are found in process monitoring and in in-built expert systems/machinability database systems designed to simplify the operation, maximize productivity and meet component workpiece surface roughness/integrity requirements[5].

Micro-EDM attracted attention from many industrial sectors such as aerospace, biomedical, defence and many more. Some examples of applications include microfluidic channels, micromold cavity[6-7], lab-on-chips, stents, miniature actuators and sensors, medical devices[8-9] inkjet printing head nozzles about 50 μm in diameter[10], micro dies and molds[11], audio resonator as muffler to reduce noise in exhaust system. EDM can also be used for machining conductive, semiconductive and even nonconductive materials. It has become one of the most viable micromanufacturing techniques for the following reasons:

1)There are almost no process forces, electrode structures can be simple which leads to filigree workpiece details with a high aspect ratio[12-13].

2)All electrically conductive materials can be machined which is a good competitiveness to other micro techniques. In addition, semiconductor and nonconductive materials can also be processed with special arrangement[14-15].

* Corresponding author. *E-mail address:* yeakub.ali@utb.edu.bn (Mohammad Yeakub ALI)
Peer review under responsibility of Editorial Committee of JAMST
DOI: 10.51393/j.jamst.2025005
2709-2135©2025 JAMST

3)Product shape complexity can even be enlarged by combining die sinking, wire EDM and other micro machining such as laser radiation, LIGA technology as well as chemical etching processes[16-17].

4)Under optimal working condition, the investment and operational cost for any variant of micro-EDM is lower than other micromachining techniques[18].

High quality micromold cavity and hot embossing master can be produced by micro-ED milling for mass replication of plastic microproducts. This process is found to be 2-5 times cost effective compared to laser and silicon micromachining[19-20]. In CNC micro-ED milling the workpiece is fed to the electrode in the designed path and materials are removed due to a series of discrete sparks occur between the workpiece and the rotating electrode[21-23].

2. Experimental work

A schematic diagram of micro-ED milling process is shown in Fig. 1. The specification of micro-ED milling machine used in this research is listed in Table 1. The process parameters include type of polarity, capacitance, gap voltage, electrode feed rate, energy threshold which are important for machining. The full understanding of micro-ED milling process parameters for nanometric surface roughness are yet to be developed, as the process itself is dynamic.

Therefore, micro-EDM is very effective to machine any two-dimensional and three-dimensional geometry parts in micrometric size with nanometric surface roughness. Micro electrodischarge (ED) milling, one of the micro-EDM variants, has this potential which has been investigated in this search.

The process parameters in micro-ED milling influence material removal rate (MRR), tool wear rate (TWR) and surface roughness where finish cut sacrifices the MRR to get minimum surface roughness. Fundamental investigation of input parameters and machinability outcome have been reported in the state of the art[8, 24]. However, literature survey has proven that there is no extensive research focusing finish cut of ED milling of to achieve nano surface quality. Hence, the objective of this research is to develope the statistical model of MRR, TWR and surface roughness R_a and R_y then find the optimal solutions of process parameters to achieve the high level machinability of titanium alloy using micro-ED milling.

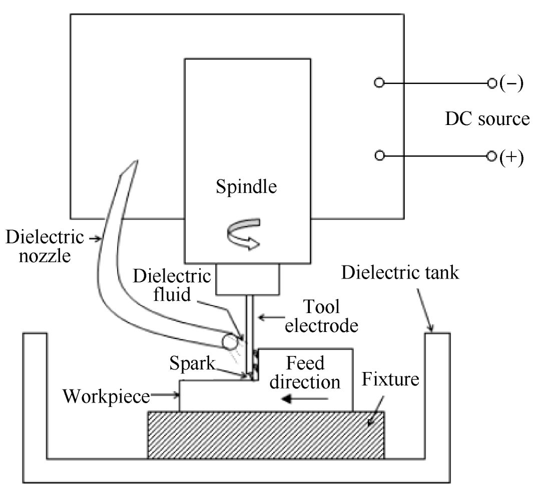

Fig. 1 Schematic micro-ED milling setup[8].

2.1. Workpiece and electrode Material

In this research titanium alloy Ti-6Al-4V workpiece and tungsten carbide electrode were used for micro-ED milling. This light weight titanium alloy is used extensively in aerospace, medical, marine, chemical engineering due to its high strength and corrosion resistance. On the other hand, tungsten carbide electrode is a superhard, wear and corrosion resistant alloy. It is also suited to make the high aspect ratio electrode for micro-ED milling and drilling. A sample of titanium alloy Ti-6Al-4V sized 17 mm×15 mm×10 mm has been ground manually using sandpaper and then polished using 3 μm diamond suspensions and lubricant liquid to get the high-quality surface for micro-ED milling process. Tungsten carbide of 0.50 mm diameter tool electrode was used to create 4 mm long and 0.50 mm deep microchannels on above mentioned workpiece.

Table 1 Specification of DT110 Micro-ED Milling machine.

Parameter	Value
Travel (mm)	X 200, Y 100, Z 100
Table working surface (mm)	350×200
T-slot configuration (mm)	6×7×25
Max spindle speed (r/min)	5000
Electrical power supply (V, Hz)	230, 50/60
Pneumatic pressure supply (MPa)	588-6867
Machine height (m)	1.9
Space (m)	1.5×1.1
Machine resolution (nm)	100

2.2. Micro-ED milling machine

The micro-ED milling processes were conducted on a multi-purpose miniature commercial machine tool known as integrated multi-process machine tool DT-110 (Fig. 2 and Table 1). This machine used resistance-capacitance (RC) circuit to discharge electrical spark. As RC circuits delivers high frequency low energy discharge, it can achieve high accuracy and surface finish.

2.3. Taguchi design of experiment

Taguchi DOE method deals with a response that is influenced by more than one input variables. It minimizes the causes of variation and reduces the number of experiments significantly. Two important aspects of Taguchi are orthogonal arrays and signal-to-noise (S/N) ratios[25]. Orthogonal arrays (OAs) are constructed in such a way that it gives a balanced design. It allows simultaneous analysis of many parameters, but it estimates the effect of each factor independent of other factors. The S/N ratio, Eq. (1) and Eq. (2), are used to evaluate the effect of an input parameter on the performance and to minimize the variability of the response while keeping the mean at desired level[26-27]. The S/N ratio is considered as “larger-the-better” Eq. (1) or “smaller-the-better” Eq.(2)[28].

$$Z = -10\lg\left(\sum_{i=1}^{n}\frac{1}{y_i^2}\Big/n\right) \tag{1}$$

$$Z = -10\lg\left(\sum_{i=1}^{n}y_i^2\Big/n\right) \tag{2}$$

where Z = S/N ratio, y_i = the observed value of the ith experiment, n = the number of repetitions for each observation.

2.3.1 Machinability assessment criteria

There are three variants of S/N ratio which are smaller-the-better, larger-the-better, and nominal-the-best. This research aims to determine the optimal micro-ED milling parameters to achieve optimum values for MRR, TWR and surface roughness R_a and R_y. Therefore, for MRR “larger-the-better” and for TWR and surface roughness “smaller-the-better” were established.

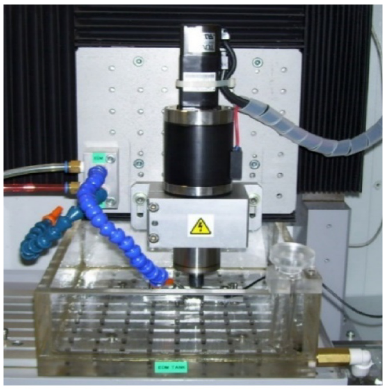

(a)

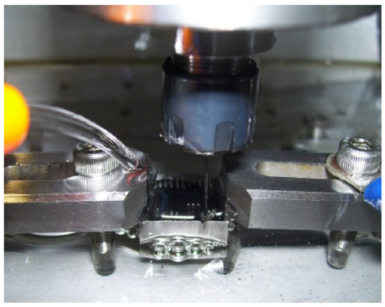

(b)

Fig. 2 (a) Micro-ED milling experiment setup, (b) magnified view of machining zone.

2.3.2 ED milling criteria

In Taguchi method, the control factors and noise factors are grouped separately. As the name, the control factor gives the stability of the design whereas the noise factors are the factors which are difficult and or expensive to control. Considering this situation, the following parameters are selected in this experimental design.

- Polarity, (+ve or -ve) of the workpiece,
- Gap Voltage, the condition of the gap to react the servo-control system,
- Capacitor to accumulate electricity and to provide electrical discharge.

These parameters were selected based on the present state of the art literature and preliminary studies. because they can potentially affect MRR and TWR and surface roughness in micro-EDM milling and be considered as to be controllable factors[8, 24]. The micro-ED milling parameters and their level are shown in Table 2. It was assumed that the tool electrode did not provide any effect to the surface roughness[29-30]. The MRR and TWR can be expressed by Eq. (3) and Eq. (4).

$$\mathrm{MRR} = \frac{\text{Material removal from workpiece}\,(\mu\text{g})}{\text{Machining time}\,(\text{s})} \tag{3}$$

$$\mathrm{TWR} = \frac{\text{Material removal from electrode}\,(\mu\text{g})}{\text{Machining time}\,(\text{s})} \tag{4}$$

3. Experimental results

Microchannels were machined on a titanium workpiece using various combination of process parameters. One of the machined microchannels is shown in Fig. 3(a). The microchannel depth profile is shown in the graph of Fig. 3(b). SEM surface micrograph of machined surface texture is shown in Fig. 3(c). Once the milling is completed, the micro-ED milling responses MRR, TWR, R_a and R_y were measured and then analyzed using Design Expert 7.1.5 (State-Ease, USA). Here the objective function is to maximize the MRR ("larger-the-better") and to minimize the TWR, R_a and R_y (smaller-the -better).

Table 2 Micro-ED milling experimental parameter.

Item	Factors	Level		
Parameter		I	II	III
Workpiece polarity	*A*	+	−	
Capacitance (nF)	*B*	1	10	100
Gap voltage (V)	*C*	80	90	100
Fixed parameters				
Workpiece	Titanium alloy (Ti-6Al-4V)			
Tool electrode	Tungsten carbide			
Electrode diameter (mm)	0.50			
Dielectric fluid	EDM-3 (synthetic oil)			
Threshold (V)	30			
Feed rate (μm/s)	2			
Spindle (r/min)	2000			

The S/N ratio is the key in the Taguchi approach to optimize the responses. The optimal set of parameters have been predicted based on optimum MRR, TWR and surface roughness (R_a and R_y).

Surface roughness, R_a and R_y for all machined channels were measured using a non-contact optical profiler Veeco Wyko NT1100. Before measuring the surface roughness, the workpiece was thoroughly cleaned with ultrasonic bath to wash away the debris that stuck on the surface. Further attempts have been made to study the surface features of channels through scanning electron microscope (JEOL JSM-5600) micrographs. MRR and TWR were measured using a high precision electronic balance (B204-S Mettler Toledo, Switzerland).

3.1. Material removal rate

MRR was analysed based on S/N ratio and ANOVA using Design Expert software. Fig. 4 shows the S/N ratio curves for MRR. It confirms that the MRR increases as the capacitance increases from 1 to 10 nF, but it slightly decreases with the change of capacitance from 10 to 100 nF. On the other hand, MRR decreases as gap voltage increases from 80 to 90 V but when it changes from 90 to 100 V, MRR increases. Finally, it indicates that the optimal combination of machining parameters for maximum MRR are 10 nF capacitance (*B*), 100 V (*C*), and negative workpiece polarity. Removing materials from titanium alloy requires frequent high energy shock. As the discharge energy is $\frac{1}{2}CV^2$, lower-level capacitance and higher-level gap voltage are needed for higher MRR.

The residual and perturbation are shown in Fig. 5 and Fig. 6 respectively while the ANOVA for MRR is shown in Table 3. The linear trend of the residuals in normal probability plot supports the condition that the error terms are normally distributed (Fig. 5). In addition, it can be seen in the perturbation plot (Fig. 6) that the factors are having steep slope or curvature which indicate that the response is sensitive. In this analysis, both capacitance (*B*) and gap voltage (*C*) are found to be affecting all the responses MRR as well as TWR, R_a and R_y.

In Table 3, the Model F-value is 23.24 implies the model is significant and there is only a 0.01% chance that an F-value 23.24 could occur due to noise. The main and interactive factors *A, B, C, BC*, are C^2 are significant as their p value is less than 0.05. The difference between predicted R^2 (0.7093) and adjusted R^2 (0.9016) is

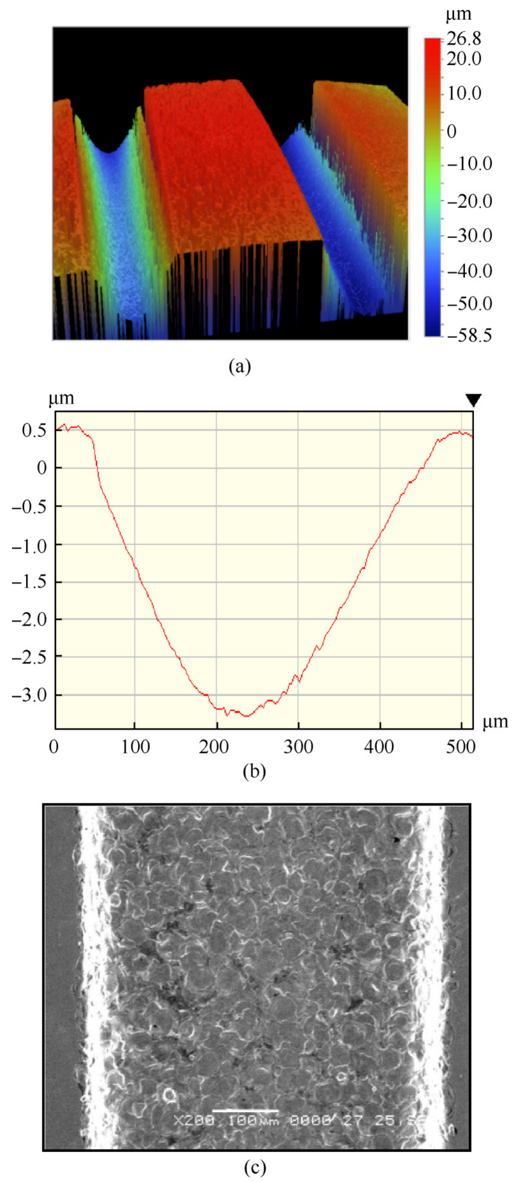

Fig. 3 (a) Wyko optical micrograph of microchannel, (b) Wyko depth profile of machined channel, and (c) SEM micrograph of machined surface texture.

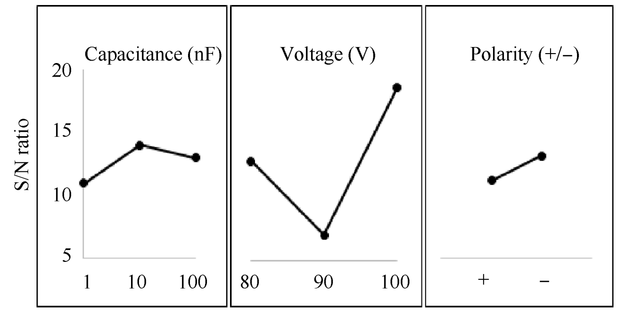

Fig. 4 S/N ratio plots for response MRR.

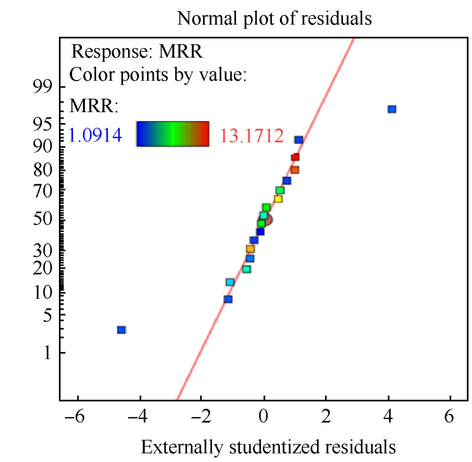

Fig. 5 Normal plot of residual of factor for the analysis of MRR.

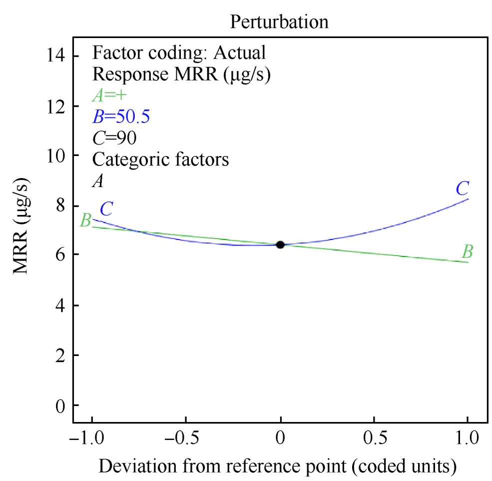

Fig. 6 Perturbation plot of factors for the analysis of MRR.

0.1923 which shows very strong agreement. Adeq precision measures the strength of signal to noise ratio where its value 4.0 and above is desirable. In this analysis the Adeq precision ratio is 14.149 and it indicates an adequate signal. Eq. (5) and Eq. (6) in terms of actual factors represent the relationship to predict MRR. Fig.7 shows the relationship between *B* and *C* as an example.

+ve polarity:

$$\mathrm{MRR}=90.64+0.577B-2.23C-0.0066BC+0.0144C^2 \tag{5}$$

−ve polarity:

$$\mathrm{MRR}=+108.2+0.63B-2.493C-0.0066BC+0.014C^2 \tag{6}$$

where MRR = material removal rate (μg/s), *B* = capacitance (nF), and *C* = gap voltage (V)

3.2. Tool wear rate

Similar to MRR, TWR has also been analysed based on S/N ratio and ANOVA. Fig. 8 shows the S/N ratio for TWR (smaller-the-better), and it confirms that the TWR decreases as capacitance increases from 1 to 100 nF. TWR also decreases as gap voltage increase from 80 to 90 V but when it changes from 90 to 100 V, the trend increases. The Fig. 8 indicates that the optimal combination of machining parameters for minimum TWR are 100 nF capacitance (*B*), 80 V (*C*), and positive workpiece polarity. As the melting point of tungsten carbide is very high (2870 °C) and the objective is to minimize TWR, lower energy discharge (lower gap voltage) is preferred. Hence the optimum parameters are considered reasonable.

ANOVA for TWR is shown in Table 4. The Model F-value 17.30 confirms that the model is significant. There is only a 0.01% chance that an F-value this large could occur due to noise. Considering the p-values less than 0.05, the model terms *A, B,* B^2 are significant. The Predicted R^2 is 0.7538 and Adjusted R^2 of 0.8519, the difference less than 0.2 showed strong agreement. Adeq precision measures the signal to noise ratio is desired to be 4.0 or higher. In

Table 3 ANOVA for surface quadratic model of MRR.

Item	SS	df	MS	F value	Prob > F
Model	253.88	7	36.27	23.24	< 0.0001 Significant
A	59.18	1	59.18	37.92	0.0001
B	5.05	1	5.05	3.24	0.0511
C	9.69	1	9.69	6.21	0.0319
AB	24.72	1	24.72	15.84	0.0026
AC	21.32	1	21.32	13.66	0.0041
BC	103.46	1	103.46	66.29	< 0.0001
C^2	8.33	1	8.33	5.34	0.0435
Residual	15.61	10	1.56		
Cor Total	269.48	17			

Std. Dev.	1.25	R^2	0.9421
Mean	5.33	Adjusted R^2	0.9016
CV(%)	23.46	Predicted R^2	0.7093
		Adeq Precision	14.1491

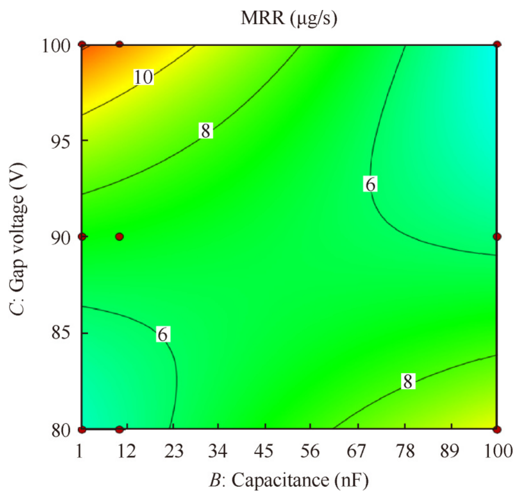

Fig. 7 MRR contour for capacitance *B* and gap voltage *C*.

this case this ratio 12.042 indicates an adequate signal.

Eq. (7) and Eq. (8) represent the relationship to predict TWR. The contour plot, Fig. 9, shows the relationship between *B* and *C* as a representative example.

+ve polarity:

$$TWR=-64.264-0.177B+1.484C+0.0016B^2-0.0082C^2 \quad (7)$$

−ve polarity:

$$TWR=-59.87-0.192B+1.483C+0.0016B^2-0.00817C^2 \quad (8)$$

where TWR = tool wear rate (μg/s), *B* = capacitance (nF) and *C* = gap voltage (V).

3.3. Average surface roughness (R_a)

Similar to MRR and TWR, R_a has also been analysed based on S/N ratio and ANOVA. Fig. 10 shows the S/N ratio for R_a. Capacitance has a very strong effect on R_a as capacitance increases from 1nF to 100 nF, R_a decreases sharply. Higher current produces higher energy discharge and diminishes sharp spikes which reduces R_a. It is also observed that R_a decreases with the increase in gap voltage. ANOVA for R_a is shown in Table 5. From F-value of 80.87, it can be confirmed that the model is perfectly significant with 99.99% confidence level. As the p-values for *B*, B^2 are below 0.05, these two model terms are significant.

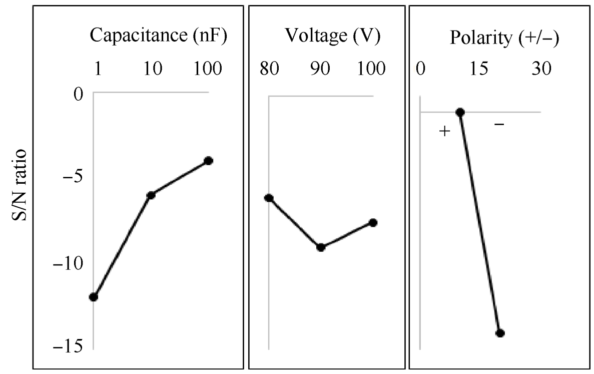

Fig. 8 S/N ratio plots for response TWR.

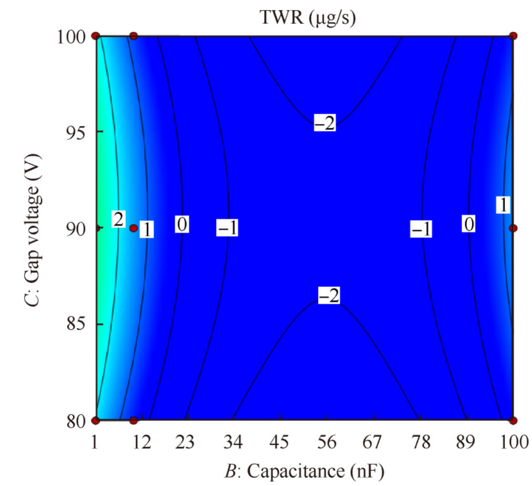

Fig. 9 TWR contour for capacitance *B* and gap voltage *C*.

Table 4 ANOVA for surface quadratic model of TWR.

Item	SS	df	MS	F value	Prob > F
Model	87.73	6	14.62	17.30	< 0.0001 Significant
A	53.91	1	53.91	63.79	< 0.0001
B	16.46	1	16.46	19.47	0.0010
C	0.1975	1	0.1975	0.2336	0.1383
AB	2.15	1	2.15	2.54	0.1393
B^2	5.46	1	5.46	6.46	0.0274
C^2	2.67	1	2.67	3.16	0.1031
Residual	9.30	11	0.8451		
Cor Total	97.02	17			

Std. Dev.	0.9193	R^2	0.9042
Mean	3.26	Adjusted R^2	0.8519
CV(%)	28.23	Predicted R^2	0.7538
		Adeq Precision	12.0416

The predicted R^2 0.9068 and adjusted R^2 0.9495; the difference is less than 0.2 showed strong agreement. Adeq precision measures the signal to noise ratio is desired to be 4.0 or higher. In this case this ratio 20.607 indicates an adequate signal. Eq. (9) in terms of actual factors represents the relationship to predict R_a. Fig. 11 shows the relationship between *B* and *C* as an example.

$$R_a=-0.0114+0.0089B+0.0016C+7.5075\times10^{-7}BC-0.00006B^2 \quad (9)$$

where R_a = average surface roughness (μm), *B* = capacitance (nF), and *C* = gap voltage (V)

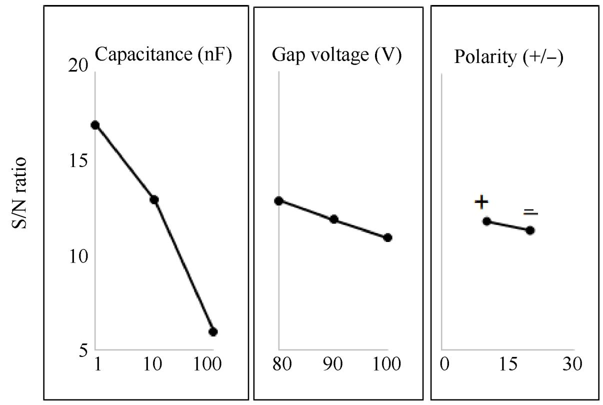

Fig. 10 S/N ratio response graph on R_a.

Table 5 ANOVA for surface roughness (R_a).

Item	SS	df	MS	F value	Prob > F
Model	0.3624	4	0.0906	80.87	< 0.0001 Significant
B	0.3267	1	0.3267	291.59	< 0.0001
C	0.0031	1	0.0031	2.76	0.1206
BC	1.351E-06	1	1.351E-06	0.0012	0.0728
*B*²	0.0066	1	0.0066	5.91	0.0303
Residual	0.0146	13	0.0011		
Cor Total	0.3770	17			

Std. Dev.	0.0335	R²	0.9614
Mean	0.2800	Adjusted R²	0.9495
CV(%)	11.95	Predicted R²	0.9068
		Adeq Precision	20.6068

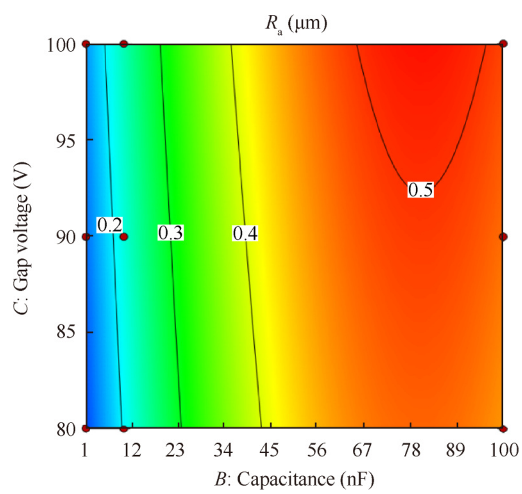

Fig. 11 R_a contour plot for capacitance *B* and gap voltage *C*.

3.4. Maximum peak-to-valley roughness (R_y)

Surface rough R_y has also been analysed based on S/N ratio and ANOVA. Fig. 12 shows the S/N ratio for R_y. Capacitance has a very strong effect on R_y as capacitance increases from 1 nF to 100 nF, R_y decreases sharply. Higher current produces higher energy discharge and diminishes sharp spikes which reduces R_y. It is also observed that R_y decreases due to the increase in gap voltage.

Model F-value 48.88 in ANOVA for R_y (Table 6) implies the model is significant. There is only a 0.01% possibility that the formulated model could be wrong. Based on p-values less than 0.05, the model terms *B* and *C* are found to be significant. The predicted R² is 0.8624 and Adjusted R² of 0.9185, the difference less than 0.2 showed strong agreement. Adeq precision measures the signal to noise ratio is desired to be 4.0 or higher. In this case this ratio 17.128 indicates an adequate signal.

Eq. (10) in terms of actual factors represents the relationship to predict R_y. The contour plot, Fig. 13 shows the relationship between *B* and *C* as an example.

$$R_y = +0.364 + 0.00977B + 0.0043C + 0.00028BC - 0.00018B^2 \quad (10)$$

where R_y = peak-to-valley surface roughness (μm), *B* = capacitance (nF), and *C* = gap voltage (V)

4. Multiple-response optimization

As multiple optimizations for all four responses were found to be with low confidence level, it is performed in two groups. The first one is for MRR and TWR as shown in Table 7. The optimum solution is found to be for positive workpiece polarity with 89.9% desirability. The optimum parameters were capacitance 100 nF and gap voltage 80 V, with optimized value of MRR 57.8 μg/s and TWR 0.96 μg/s. The result of experimental validation, as shown in Table 8, showed that the error is below 10%. So, the developed model is significant. The second optimization is for R_a and R_y as shown in Table 9 for positive polarity.

The experimental validation, as shown in Table 10, showed that the errors for R_a and R_y are 10% and 8% respectively. Therefore, the optimum machining parameters for minimum R_a and R_y are capacitance 1 nF, and gap voltage 80 V and with optimized value of R_a 0.086 μm and R_y 0.63 μm.

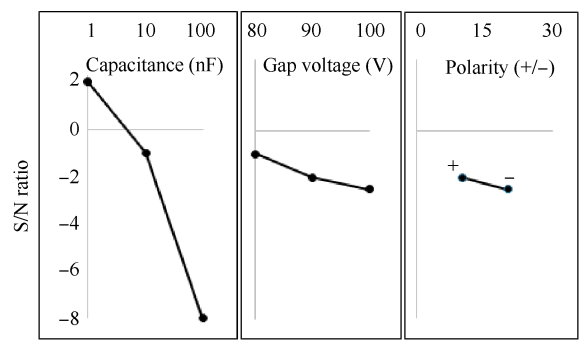

Fig. 12 S/N ratio response graph on R_y.

Table 6 ANOVA for surface roughness (R_y).

Item	SS	df	MS	F value	Prob > F
Model	9.91	4	2.48	48.88	< 0.0001 Significant
B	8.32	1	8.32	164.12	< 0.0001
C	0.3706	1	0.3706	7.31	0.0180
BC	0.1875	1	0.1875	3.70	0.0766
*B*²	0.0690	1	0.0690	1.36	0.2641
Residual	0.6588	13	0.0507		
Cor Total	10.57	17			

Std. Dev.	0.2251	R²	0.9377
Mean	1.43	Adjusted R²	0.9185
CV(%)	15.70	Predicted R²	0.8624
		Adeq Precision	17.1284

Table 7 Multiple optimizations for MRR and TWR.

A	*B*	*C*	MRR	TWR	Desirability(%)
+	100	80	57.80	0.959	89.9
−	10	100	63.66	5.970	52

Table 8 Comparison of predicted and actual MRR and TWR.

Responses	Predicted	Actual	Error(%)
MRR (μg/s)	57.8	53.28	8.5
TWR (μg/s)	0.96	1.06	9.5

Table 9 Multiple optimization solution for R_a and R_y.

A	*B*	*C*	R_a	R_y	Desirability(%)
+	1	80	0.086	0.631	99

Table 10 Comparison of predicted and actual R_a and R_y.

Responses	Predicted	Actual	Error(%)
R_a (μm)	0.086	0.095	10.05
R_y (μm)	0.631	0.581	8.06

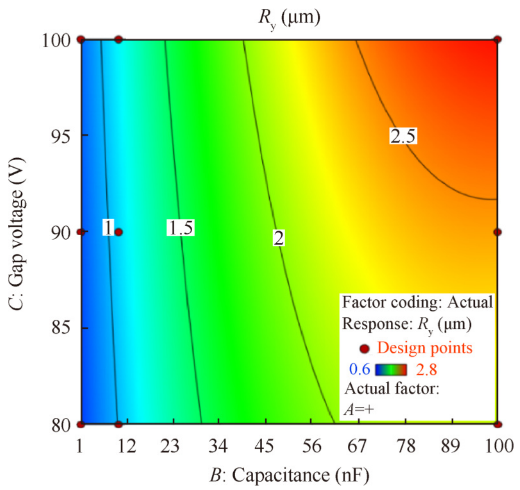

Fig. 13 R_y contour plot for capacitance *B* and gap voltage *C*.

5. Conclusions

This paper discusses the machinability of titanium alloy Ti-6Al-4V using micro-ED milling. The main target was high MRR, low TWR, and lower surface roughness R_a and R_y. Experiments are based on Taguchi orthogonal array of micro-ED milling parameters polarity, capacitance, and gap voltage. From these set of experimental and ANOVA investigations, the following conclusions were drawn:

1)The ANOVA analysis showed that the MRR model is significant. Factor *A* (polarity) and *C* (Gap Voltage) are found to be significant also. Although capacitance Factor *B* (capacitance) is found to be less significant, as it is one of the main parameters and it is included in the model equation. Several two factor ineractions are also found to be significant model terms.

2)From S/N ratio analysis, the optimal combination levels of micro-ED milling parameters for maximum MRR are 10 nF capacitance, 100 V gap voltage. For minimum TWR, the optimal combination of parameters is 1 nF capacitance and 80 V gap voltage.

3)Below 10% errors were identified for both MRR and TWR. It shows that the developed mathematical models are significant to represent the relationships and useful to predict the performance of micro-ED milling process.

4)Optimal micro-ED milling process parametric combinations are found to be 1 nF capacitance, 80 V gap voltage for surface roughness, R_a and R_y.

5)The developed R_a and R_y models are significant to represent the predicted relationships and useful to predict surface roughness without real life experiment.

6)The effect of polarity is difficult to quantify as it varies depending on workpiece material, tool material and machining parameters. As titanium alloy is difficult to dissolve (melting point 1725 °C) by heat, it is better to apply thermal shock with positive polarity. If the objective is to remove bulk material, then also the workpiece polarity should be positive. If an ultra-finish surface is required, the workpiece polarity should be negative. However, in such as a case the tool electrode is to be replaced more frequently.

7)From the observation of SEM micrographs, it is seen that the edge of channel shows many burrs and there are no consistencies of pattern profile of the channel. Future study should be done to tackle this issue.

Acknowledgements

The authors are thankful to the technical staff in Tool and Die Laboratory at International Islamic University Malaysia for allowing experimental works.

References

1. Wu B, Cao YX, Xu B, et al. Micro-milling of 3D micro-electrode and its application in 3D micro-EDM. *Int J Adv Manuf Technol* 2024;132 (11-12):5597-5607.
2. Kumar M, Datta S, Kumar R. Electro-discharge machining performance of Ti-6Al-4V alloy: studies on parametric effect and phenomenon of electrode wear. *Arab J Sci Eng* 2019; 44(2):1553-1568.
3. Rathod R, Kamble D, Ambhore N. Performance evaluation of electric discharge machining of titanium alloy-a review. *J Eng Appl Sci*, 2022; 69:64.
4. Abbas NM, Solomon DG, Bahari MF. A review on current research trends in electrical discharge machining (EDM). *Int J Mach Tools Manuf* 2007; 47(7-8):1214-1228.
5. Hou S, Bai J, Liu H. Improving performance of micro-hole EDM based on frequency detection method. *Int J Adv Manuf Technol* 2022; 121(5-6):3259-3270.
6. Ali MY, Atiqah N. Silicon carbide powder mixed micro electro discharge milling of titanium alloy. *Int J Mech Mater Eng* 2012;6(3):338-342.
7. Sarma P, Patowari PK. Fabrication of metallic micromixers using WEDM and EDM for application in microfluidic devices and circuitries. *Micro Nanosyst* 2018;10(2):137-147.
8. Mehfuz R, Ali MY. Investigation of machining parameters for the multiple-response optimization of micro electrodischarge milling. *Int J Adv Manuf Technol* 2008;43(3):264-275.
9. Yuan S, Hung NP, Ngoi BKA, et al. Development of microreplication process-micromolding. *Mater Manuf Process* 2003;18(5):731-751.
10. Sivaprakasam P, Prakash JU, Hariharan P, et al. Micro-electric discharge machining (Micro-EDM) of aluminium alloy and aluminium matrix composites-a review. *Adv Mater Process Technol* 2021; 8(2): 1699-1714.
11. Qudeiri JEA, Zaiout A, Mourad AHI, et al. Principles and characteristics of different EDM processes in machining tool and die steels. *Appl Sci* 2020;10(6):2082.
12. Singh NK, Pandey PM, Singh KK, et al. Steps towards green manufacturing through EDM process: A review. *Cogent Eng* 2016; 3(1): 1272662.
13. Chatterjee S, Das S. Micro-electric discharge machining in standard setup. In: Srichand H, Kuang-Chao F, editors. *Proceedings of the 35th International MATADOR Conference*; 2007 Jul; 2007. p.77-80.

14. Banu A, Ali MY, Rahman MA, et al. Stability of micro dry wire EDM: OFAT and DOE method. *Int J Adv Manuf Technol* 2020; 106(9-10): 4247-4261.
15. Zhu X, Li G, Mo J, et al. Electrical discharge machining of semiconductor materials: A review. *J Mater Res Technol*, 2023; 25(Jul-Aug): 4354-4379.
16. Li Z, Bai J, Cao Y, et al. Fabrication of microelectrode with large aspect ratio and precision machining of micro-hole array by micro-EDM. *J Mater Process Technol* 2019;268(June):70-79.
17. Zhou T, He Y, Wang T, et al. A review of the techniques for the mold manufacturing of micro/nanostructures for precision glass molding. *Int J Extreme Manuf* 2021;3(4):042002.
18. D'Urso G, Giardini C, Quarto M, et al. Cost index model for the process performance optimization of micro-EDM drilling on tungsten carbide. *Micromachines* 2017; 8(8), 251.
19. Ali MY, Mohammad AS. Effect of conventional EDM parameters on the micromachined surface roughness and fabrication of a hot embossing master microtool. *Mater Manuf Process* 2009;24(4):454-458.
20. Kuo CC, Chiang TS. Development of a precision hot embossing tool with microstructures for microfabrication. *Int J Adv Manuf Technol* 2017;91(1-4):1321-1326.
21. Pham HV, Nguyen HP, Shailesh S, et al. Investigating technological parameters and TiN-coated electrodes for enhanced efficiency in Ti-6Al-4V micro-EDM machining. *Metals* 2024;14(2):162.
22. Ali MY, Hamad MH, Karim AI. Form characterization of microhole produced by microelectrical discharge drilling. *Mater Manuf Process* 2009;24(6):683-687.
23. Vidya S, Vijay BS, Chebolu A, et al. Effects of different cavity geometries on machining performance in micro-electrical discharge milling. *J Micro Nano Manuf* 2015;3(1):011007.
24. Bigot S, Valentincic J, Blatnik O, et al. Micro-EDM parameters optimization. In: Stefan D, Wolfgang M, Bertrand F, editors. 4M 2006: *Proceedings of the 2nd International Conference on Multi-Material Micro Manufacture;* 2006 Sep 20-22; Grenoble, France: Elsevier; 2006. p.195-198.
25. Durakovic B. Design of experiments application, concepts, examples: State of the art. *Period Eng Nat Sci* 2017;5(3):421-439.
26. Bellotti M, Qian J, Reynaerts D. Process fingerprint in micro-EDM drilling. *Micromachines* 2019;10(4):240,1-15.
27. Sulaiman MA, Haron CH, Ghani JA, et al. Optimization of turning parameters for titanium alloy Ti-6Al-4V using the response surface method. *Int J Adv Manuf Technol* 2013;7(2):11-28.
28. Pradhan BB, Masanta M, Sarkar BR, et al. Investigation of electro-discharge micro-machining of titanium super alloy. *Int J Adv Manuf Technol* 2008;41(11-12):1094-1106.
29. Sahu AK, Mahapatra SS. Surface characteristics of EDMed titanium alloy and AISI 1040 steel workpieces using rapid tool electrode. *Arab J Sci Eng* 2020;45(2):699-718.
30. Shastri RK, Mohanty CP. Sustainable electrical discharge machining of Nimonic C263 superalloy. *Arab J Sci Eng* 2021;46(8):7273-7293.